THE JOURNAL OF PHYSICAL CHEMISTRY C

Article

Cite This: J. Phys. Chem. C 2019, 123, 9764–9769

pubs.acs.org/JPCC

Electron Confinement Effects in Silver Films Embedded between Graphene and Metallic Substrates

L. Ferrari,[†] I. Grimaldi,[‡] P. M. Sheverdyaeva,[¶] Asish K. Kundu,[§] P. Moras,[¶] M. Papagno,[‡] C. Carbone,[¶] and D. Pacilè*[,‡]

[†]Istituto di Struttura della Materia, Consiglio Nazionale delle Ricerche, 00133 Roma, Italy

[‡]Dipartimento di Fisica, Università della Calabria, 87036 Arcavacata di Rende (CS), Italy

[¶]Istituto di Struttura della Materia, Consiglio Nazionale delle Ricerche, 34149 Trieste, Italy

[§]International Center for Theoretical Physics (ICTP), 34151 Trieste, Italy

Supporting Information

ABSTRACT: We examine the electronic structure of Ag deposits intercalated between graphene and Co(0001). Angle-resolved photoemission spectroscopy measurements reveal the formation of Ag sp-derived quantum well states due to finite electron reflectivity across the buried metal/metal interface. This observation provides evidence of flat Ag(111) film growth underneath graphene, in analogy with the layer-by-layer growth of Ag on the corresponding graphene-free surfaces. Band dispersion and spectral properties of the quantum well states reflect primarily the interaction with the supporting substrate. Signatures of the coupling between graphene and the underlying films are the shift of the Ag(111) surface state, the hybridization gap opening of the π state crossing the Ag 4d states, the downward shift of the Dirac point (n-type doping), and the gap between π and π^* Dirac cones. Similar observations are reported for Ag(111) films intercalated between Gr and Pt(111). These systems can be considered as prototypes of graphene-protected thin metal films displaying electron confinement effects.

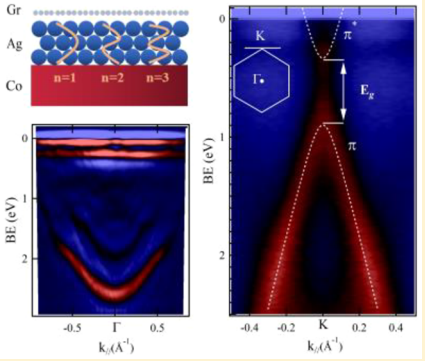

INTRODUCTION

The formation of discrete quantum well (QW) states in thin metal films on supporting substrates can be easily understood in terms of the particle-in-a-box picture.[1,2] The film boundaries, i.e., the interface and the film surface, define a one-dimensional potential well of width corresponding to the film thickness. The valence electrons of the films can acquire a standing wave character and present a discrete QW energy spectrum under two conditions. First of all, an ordered film of uniform thickness is required. To this end, optimized growth conditions (deposition rate, temperature, absence of contaminants, etc.) are necessary to get clean and flat films over large areas of the substrate. Second, the electron reflectivity at the interface must be different from zero. This condition avoids full propagation of the electron waves into the bulk of the supporting material. It was shown that even for closely matched materials (Ag and Au), a reflectivity of few percent leads to observable effects of electron confinement.[3,4]

Microscopic methods, such as scanning tunneling spectroscopy[5,6] and low-energy electron microscopy,[7] can reveal the presence of discrete QW states in films of reduced lateral dimensions (a few tens of nanometers) with limited momentum resolution. Complementarily, angle-resolved photoemission spectroscopy (ARPES) provides high energy and momentum resolutions at once, but averages over few to hundreds of micrometers (mainly depending on the optical focusing of the photon beam). Therefore, the growth of atomically flat films on large areas of the substrate is a primary task for the study of electron confinement effects by ARPES. Indeed, many sp- and d-like metal films, grown according to optimized procedures, display well-defined QW state peaks in ARPES spectra. Conversely, the coexistence of multiple film thicknesses (and/or roughness) over the area scanned by ARPES results in ill-defined confinement conditions and broad spectral features.[8]

From these premises, the intercalation of metals underneath a graphene (Gr) layer appears as an uncertain method for the creation of flat films and observation of electron confinement effects by ARPES. In fact, the intercalation process involves mass transport through defects of the Gr layer and should favor an inhomogeneous film growth. So far, experimental studies examined the intercalation of thin metal films underneath a Gr layer with microscopic and surface sensitive probes.[9−15] For instance, scanning tunneling microscopy/spectroscopy pointed out the weak interaction of intercalated Ag(111) or Au(111) films with ordered Gr flakes.[13−15] At present, specific information about the properties of deeper lying layers of the metal is not available.

Received: October 11, 2018
Revised: March 29, 2019
Published: March 29, 2019

DOI: 10.1021/acs.jpcc.8b09935
J. Phys. Chem. C 2019, 123, 9764–9769

In the present study we analyze by ARPES the electronic structure of Ag films intercalated in the Gr/Co(0001) interface, and compare the results with those obtained for the bare Ag/Co(0001) interface. The observation of Ag sp-derived QW states demonstrates that intercalation is a viable route for the production of atomically uniform Ag(111) films in contact with Gr. Similar results are obtained by Ag intercalation in the Gr/Pt(111) system. The interaction of these materials gives rise to a large $\pi-\pi^*$ gap located several hundreds meV below the Fermi level (E_F), and a hybridization gap between π and Ag 4d levels. Beside the fundamental interest of these findings, the creation of uniform films with well-defined electronic states may simplify the understanding of the electron transport properties across the Gr/metal contact interface. Moreover, many physical properties (among them transport properties) and ultimate applications require surfaces that are exposed to ambient environment (1 atm and room temperature). One critical issue is then how the thin films will behave under such ambient conditions. While this problem has been overcome in selected semiconductor heterostructures,[16] it is certainly still open for thin metal films. In this respect, thanks to the Gr passivation efficiency, the present study may offer the opportunity to transfer the longstanding expertise on QW states of noble metal thin films in application research areas.

METHODS

The experiments were carried out at the VUV-photoemission beamline of the Elettra synchrotron radiation facility in Trieste.[17] A thick Co film (5−6 nm) was grown on W(110) by evaporation of Co on the clean substrate at room temperature followed by a postannealing to approximatively 420 K. Ag films on bare Co(0001) were grown using a resistively heated drop on a tungsten filament, with the substrate kept at 80 K and successively annealed at room temperature, to favor the formation of layers with atomically uniform thickness. Due to the lattice mismatch (13.1%; a_{Co} = 2.51 Å and a_{Ag} = 2.89 Å are the nearest neighbor distances), few-layers Ag films display a moiré superstructure with the axis aligned to the main directions of Co(0001), as seen in Figure 1a (right panel). Above six monolayers (ML) (1 ML = 2.36 Å) the (1 × 1) of Ag(111) is recovered in the low-energy electron diffraction (LEED) pattern. The Gr/Ag/Co system was prepared by Ag intercalation in Gr on thick Co(0001) films, as described elsewhere.[11] Ag was evaporated on top of the Gr layer at room temperature. The sample was repeatedly annealed at about 700 K, for a total time of about 30 min, leading to the formation of Gr on Ag(111), as previously reported.[14,15] The intercalation process was monitored by core levels and valence band spectra. Representative XPS data are reported in Figure S1a (Supporting Information). ARPES measurements were performed at 18 K using a R-4000 Scienta electron analyzer, which allows parallel acquisition over 30° angular range. Photon energies of 55 and 120 eV were chosen to enhance selectively the intensities of Ag sp-QW states and Gr bands. Energy and angular resolution were set to 15 meV and 0.3°, respectively.

The Pt(111) crystal was prepared by repeated Ar^+ sputtering at 1.5 keV of beam energy and high temperature flash-annealing cycles in oxygen atmosphere, until a sharp (1 × 1) LEED pattern and well-developed core level components (Figure S1b) were observed. The Gr layer was grown by exposing the Pt(111) surface to a partial pressure of 5 × 10^{-7} mbar of ethylene, with the temperature kept at about 1100 K in order to grow the $(\sqrt{3} \times \sqrt{3})$R30° Gr domain.[18,19] The intercalation of Ag deposits on Gr/Pt(111) was achieved as described for the Co substrate.

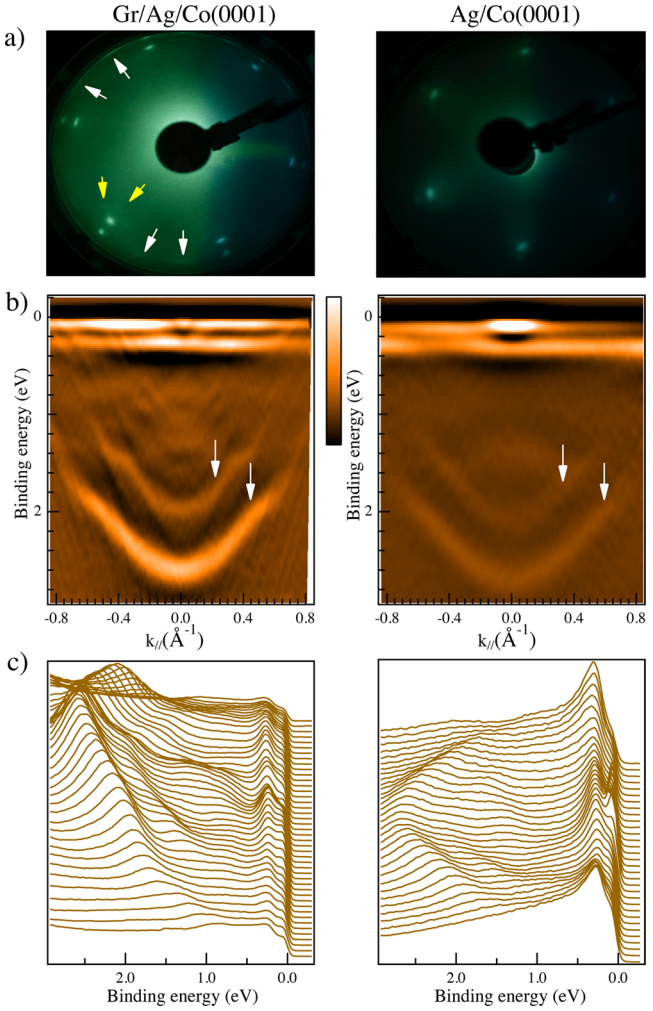

Figure 1. (a) LEED images (110 eV primary energy): (left panel) the (7 × 7)/(6 × 6) moiré superstructure of Gr on a Ag film grown on Co(0001), where yellow arrows indicate the spots of the superstructure, while white ones indicate Gr multidomains; (right panel) the moiré superstructure of a Ag film of 2.5 ML thickness grown on Co(0001). (b) Second derivative photoemission intensity plots, taken with photon energy of 55 eV and centered at $\bar{\Gamma}$: (left panel) Gr/2.5MLAg/Co(0001); (right panel) 2.5MLAg/Co(0001). White arrows highlight Ag sp-QW states. (c) Energy distribution curves extracted from measurements of Figure 1b: (left panel) Gr/2.5MLAg/Co(0001); (right panel) 2.5MLAg/Co(0001).

RESULTS AND DISCUSSION

The structural properties of Gr on intercalated Ag multilayers have been reported in the literature.[14] Due to the mismatch between the planar lattice constants of Gr and Ag(111) (14.9%; a_{Gr} = 2.46 Å, a_{Ag} = 2.89 Å), a (7 × 7)/(6 × 6) moiré structure with a periodicity of 16.4 Å has been observed. Indeed, this superstructure of Gr on Ag multilayers is present in Figure 1a (left panel, see below for description). We have performed the intercalation of Ag using two different substrates, Gr/Co(0001) and Gr/Pt(111).

DOI: 10.1021/acs.jpcc.8b09935
J. Phys. Chem. C 2019, 123, 9764−9769

The electronic structure of Gr/Co(0001) has been characterized by ARPES in previous studies.[11,20] Starting from a Gr/Co interface, we intercalated Ag multilayers by the annealing procedure described above. Figure 1a (left panel) shows the corresponding LEED image, where the inner spots belong to Ag and outer ones to Gr, while weak azimuthally elongated spots, highlighted by white arrows, indicate a multidomains Gr superstructure. In Figure 1b (left panel) we show the resulting electronic band structure of Gr/Ag(111)/Co(0001) around $\bar{\Gamma}$, taken with a photon energy of 55 eV. The main features of Figure 1b (left panel), highlighted by white arrows, are Ag sp-derived QW states, arising from the intercalated Ag film. In free-standing Ag(111) films, QW states would appear with parabolic dispersion, more packed to each other and closer to E_F as the film thickness increases. If Ag films are grown on single-crystals,[21−23] hybridization effects with the surface-projected bands of the substrate modify the ideal behavior in specific regions of the energy-momentum space. In order to catch the similarity with Ag sp-derived QW states on Co(0001) and to quantify the number of intercalated layers, we report in Figure 1b (right panel) the ARPES measurements of 2.5 ML Ag film grown on the bare substrate. The deeper QW state, with minimum at about 2.64 eV, would be the only seen for a thickness of 2 ML (see Figure S2a), while the higher one, with minimum at about 2.12 eV, is characteristic of 3 ML uniform coverage, as also deduced from comparison with existing literature on Ag/Ni(111).[24] Therefore, the number of Ag QWs seen in Figure 1b (left panel), their parabolic trend, and binding energy position are comparable to the results obtained for a Ag coverage on bare Co(0001) between 2 and 3 ML. Weaker QWs with minimum between 1.2 and 1.4 eV, detected in Figure 1b (left panel), are signature of regions with a higher number of intercalated layers, as also deduced by selected experiments on bare Co(0001) (Figure S2b). However, considering that the typical coherence length required to observe QWs is in the order of 50 Å, we assume that there are mainly homogeneous and flat regions of 2 or 3 ML of the Ag film, each of which must have this minimum size. Moreover, by comparing ARPES results, we attribute the nondispersing state close to E_F in Figure 1b (left panel) to Co 3d bands. Interestingly, the comparison also shows the shift of the surface state in Gr/Ag/Co, which is expected for Ag(111) single-crystal upward-dispersing around $\bar{\Gamma}$, with a minimum at about 67 meV at 5 K.[25,26] In Ag films grown on bare Co(0001) the surface state is the most prominent feature observed across E_F, dispersing around $\bar{\Gamma}$ within $k = \pm 0.15$ Å^{-1}, as seen from Figure 1c (right panel). Several studies have shown that the adsorption of Gr on weakly interacting metals (i.e., Pt, Ir, Au) preserve the surface states.[10,27] The shift of the Ag surface state in the present system is in agreement with previous STM/STS studies on Gr/15MLAg/Ir(111),[12] reporting a shift above E_F (from −0.075 eV up to 0.011 eV) upon intercalation of Ag film underneath the Gr layer. Therefore, we interpret the small intensity at $\bar{\Gamma}$ near E_F as the tail of the surface state, as seen from Figure 1c (left panel). This shift toward unoccupied states has been explained as due to two combined factors: from one side the epitaxial strain of the Ag lattice constant, in analogy with the growth of Ag films on dissimilar bare substrates;[28,29] on the other side, the perturbation introduced by the Gr layer in changing the boundary conditions. Similar results have been reported later for Gr/Ag/Ir(111) by STS investigation.[14] Uncovered Ag films on Ir(111) exhibit already a shift above E_F of the surface state, which is further increased in Gr-covered regions. For the present system, we can rule out that the effect of strain is responsible of the shift, as Ag films on bare Co(0001) exhibit the surface state below E_F. Therefore, the interaction of the Gr layer on Ag multilayers is strong enough to change the surface potential, in analogy with the adsorption of Xe on Ag(111), for which an upward shift from −67 to +52 meV of the surface state has been measured.[30]

To shed light on the role of the supporting substrate, we have performed similar experiments on Ag multilayers intercalated in Gr/Pt(111) (Figure S3). In analogy with the trend observed on bare Pt(111),[21] Figure S3a shows Ag sp-derived QW states arising from the intercalated multilayers Ag film, labeled with quantum numbers n. By comparing the position of QW states with existing literature,[21] we estimate a film thickness of about 18 Ag ML. Analogies with the bare Ag/Pt interface are a flat bottom for first bands, together with a significative lowering of spectral weight at higher binding energy, in a triangular region around $\bar{\Gamma}$, due to hybridization effects with the surface-projected bands of the substrate. The deviation from a parabolic dispersion of $n = 4$ and $n = 5$ bands is also due to the presence of a poorly reflecting region. Moreover, the sequence of energy distribution curves (EDCs) of Figure S3b shows the absence of the Ag surface state, in analogy with the results discussed above for Gr/Ag/Co(0001).

By comparing the experiments here reported using Co (Figure 1) and Pt substrates (Figure S3), we conclude that Ag multilayers intercalated on Gr recall the growth properties on the bare substrate, and thus energy-dispersion curves of QWs mainly reflect the supporting metal rather than the Gr layer on top. Consequently, a Gr-protected film is achievable on different supporting metals.

Finally, we move the attention to the electronic properties of Gr on intercalated Ag multilayers. In Figure 2a, we report a wide photoemission intensity plot taken at 120 eV of photon energy, along $\bar{\Gamma}\bar{K}$ of main domains of Gr/Ag/Co, showing Gr π and σ states and Ag 4d bands. The good crystalline quality of Ag films is proved by the appearance of dispersive 4d Ag states. We notice that the decoupling of the Gr layer from the Co substrate is proved by the minimum of the π state at the $\bar{\Gamma}$ point, found here at 8.72 eV, against 10.10 eV reported for Gr/Co(0001).[11] However, according to a previous investigation where a considerable Gr-Ag interaction has been detected,[31] we confirm here a significant hybridization between the Gr π band and Ag 4d bands, resulting in the formation of a band gap, centered at about 4.5 eV of binding energy in the present experiment. This finding has been highlighted in the inset of Figure 2a, reporting the first derivative of the ARPES data enclosed by a dashed line, where the band gap has been indicated within a white circle. In parts b and c of Figure 2, photoemission intensity plots showing the n-doped π and π^* Dirac cones in proximity of E_F are reported, along main $\bar{\Gamma}\bar{K}$ and orthogonally to it, respectively. The doping effect and band gap opening of epitaxial noble-metal contacts on Gr has been widely discussed in the literature within different first-principles DFT calculations.[32−34] Taking into account a physisorbed Gr layer located at large distance (d = 5 Å) from a metal surface, one would expect a rigid charge transfer from the metal to Gr, or in the opposite direction, only due to the difference of corresponding work functions (W). Specifically, since W_{Ag} = 4.92 eV, and W_{Gr} = 4.60 eV, the Gr/Ag interface is expected to be close to the neutral point at large distance, with a slight p-doping. Actually, at a typical

DOI: 10.1021/acs.jpcc.8b09935
J. Phys. Chem. C 2019, 123, 9764−9769

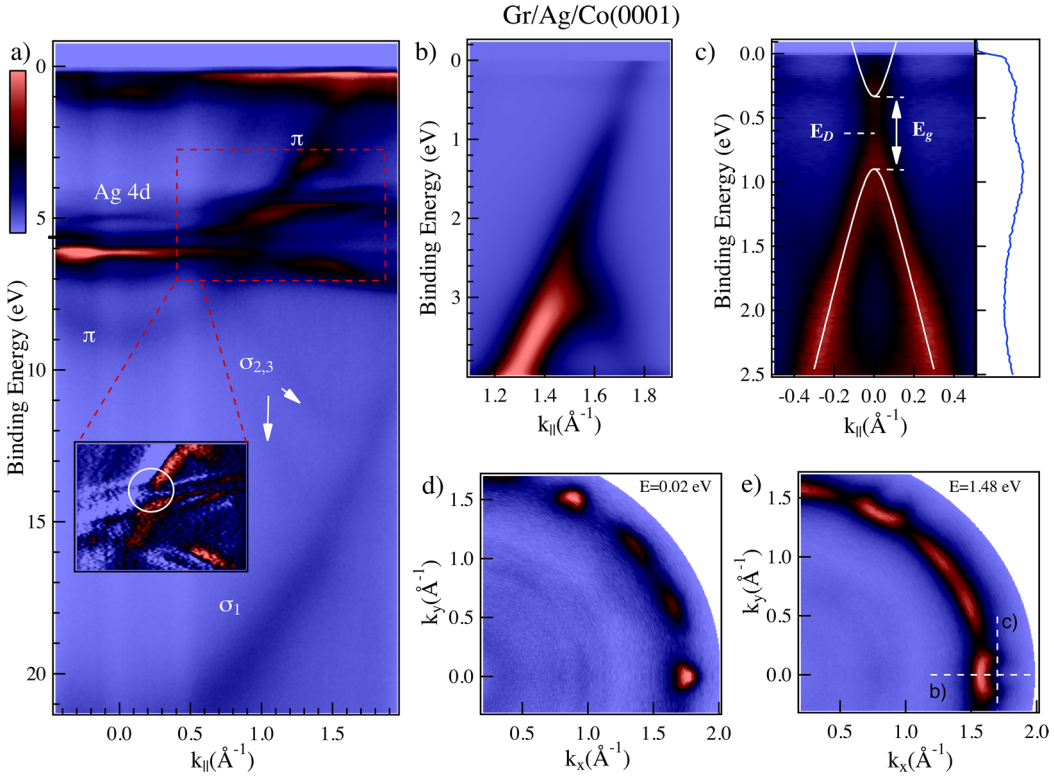

Figure 2. ARPES measurements taken on Gr/Ag/Co(0001). (a) Extended photoemission intensity plot along main $\bar{\Gamma}\bar{K}$ of Gr, taken at 120 eV of photon energy. The inset shows the first derivative of the region enclosed by dashed lines. (b and c) Photoemission intensity plots taken at 55 eV of photon energy, along main $\bar{\Gamma}\bar{K}$ of Gr and perpendicularly to it, respectively. On the right side of panel c, the energy distribution curve extracted at k = 0 from part c is reported. (d and e) Constant-energy maps taken 0.02 eV below E_F, and at 1.48 eV of binding energy, respectively. In part e, dashed lines indicate the directions along which parts b and c are taken.

equilibrium separation of d = 3.3 Å for weakly interacting metals, there is also a contribution coming from the overlap integral between wave functions of metal and Gr, which can account for the failure of a simple picture of charge transfer.

In the present experiment, the linear extrapolation of the π and π^* band dispersions toward the $\bar{K}$ point do not overlap (Figure 2b,c). They are misaligned along the momentum axis and separated by a depression of the photoemission intensity, giving a clear signature of an energy band gap. The anomalous behavior near the Dirac point of epitaxial Gr has been first observed on SiC(0001), and through a controversial interpretation of data, it has been inferred to electron-plasmon scattering[35] or symmetry breaking caused by substrate bonding.[36] A gap-like spectrum was also seen in disordered Gr, leading to the information that a high number of defects or small Gr domain size broaden the intrinsic spectral function.[37−39] Energy gaps partially hidden by nonvanishing intensity have been observed in other intercalated Gr-systems,[40,41] first discussed for Gr/Au(1 ML)/Ru(0001) and ascribed to the breaking of the C sublattice symmetry.[42] Focusing here on Gr/Ag systems, previous ARPES studies showed that Gr on one interlayer of Ag(111) becomes heavy electron doped, with a Dirac point (E_D) located at (400 ± 100) meV and a band gap (E_g) of (450 ± 100) meV when Re(0001) is used as supporting substrate[31] and with E_D=(560 ± 5) meV and E_g = (320 ± 5) meV on Ni(111).[41] The present system differs for the number of Ag interlayers, the supporting substrate, and thus the Gr superstructure. However, from the photoemission intensity plot taken along the direction perpendicular to the main $\bar{\Gamma}\bar{K}$ axis of Gr (Figure 2c), and from EDC extracted at the center of the Dirac cones, we estimate for Gr/Ag/Co(0001) E_D = (620 ± 15) meV and E_g = (560 ± 15) meV, which are in agreement with STS results for Gr/Ag(111),[14] reporting E_D = (560 ± 80) meV. A similar trend has been observed using Pt(111) as a supporting substrate (Figure S4). Moreover, in parts d and e of Figure 2, photoemission measurements of constant-energy surface close to E_F, and down to 1.48 eV binding energy, are displayed. At the Fermi surface, red spots located at the main $\bar{K}$ points correspond to constant energy cuts of the π^* band of Gr. Weaker π^* bands located at (20 ± 1)° and (40 ± 1)° are originated from rotated Gr domains. At higher binding energy (Figure 2e), one notes characteristic triangular contour of π band of Gr for the main domain, fully described within the tight-binding approach,[43] and a spread of the signal along circular segments for rotated domains. Notably, in both constant energy cuts, faint inner circles visible within $|k| \simeq 1.00$ Å^{-1} correspond to Ag sp-derived QW states.

CONCLUSIONS

In this work, we have investigated by means of ARPES the electronic structure of Ag multilayers intercalated between Gr and selected transition metals. We provide evidence that the intercalation of Ag multilayers on selected transition metals is a well-ordered process across the film, similarly to a layer-by-layer growth on bare metals. The flat thin film embedded between Gr and the Ag-metal interface yields electron confinement effects, resulting in well-defined quantum well states, strongly dependent on the overlap integrals with the band structure of the substrate. Moreover, concerning the

DOI: 10.1021/acs.jpcc.8b09935
J. Phys. Chem. C 2019, 123, 9764−9769

electronic structure of Gr, we provide evidence, for the first time by ARPES, of *n*-doping and band gap opening between π and π^* Dirac cones of Gr on multilayers Ag films.

■ ASSOCIATED CONTENT

Supporting Information

The Supporting Information is available free of charge on the ACS Publications website at DOI: 10.1021/acs.jpcc.8b09935.

Representative XPS measurements of Gr/Ag/Co(0001) and Gr/Ag/Pt(111) and ARPES measurements of Ag/Co(0001) and Gr/Ag/Pt(111) (PDF)

■ AUTHOR INFORMATION

Corresponding Author

*(D.P.) E-mail: daniela.pacile@fis.unical.it.

ORCID

P. M. Sheverdyaeva: 0000-0002-4231-1638

D. Pacilè: 0000-0001-6219-3889

Notes

The authors declare no competing financial interest.

■ ACKNOWLEDGMENTS

A.K.K. acknowledges the receipt of a fellowship from the ICTP-TRIL Programme, Trieste, Italy.

■ REFERENCES

(1) Chiang, T.-C. Photoemission Studies of Quantum Well States in Thin Films. *Surf. Sci. Rep.* **2000**, *39*, 181−235.

(2) Milun, M.; Pervan, P.; Woodruff, D. P. Quantum Well Structures in Thin Metal Films: Simple Model Physics in Reality? *Rep. Prog. Phys.* **2002**, *65*, 99−141.

(3) Topwal, D.; Manju, U.; Pacilé, D.; Papagno, M.; Wortmann, D.; Bihlmayer, G.; Blügel, S.; Carbone, C. Quantum Electron Confinement in Closely Matched Metals: Au Films on Ag(111). *Phys. Rev. B: Condens. Matter Mater. Phys.* **2012**, *86*, 085419.

(4) Sheverdyaeva, P. M.; Requist, R.; Moras, P.; Mahatha, S. K.; Papagno, M.; Ferrari, L.; Tosatti, E.; Carbone, C. Energy-Momentum Mapping of d-Derived Au(111) States in a Thin Film. *Phys. Rev. B: Condens. Matter Mater. Phys.* **2016**, *93*, 035113.

(5) Wegner, D.; Bauer, A.; Kaindl, G. Electronic Structure and Dynamics of Quantum-Well States in Thin Yb Metal Films. *Phys. Rev. Lett.* **2005**, *94*, 126804.

(6) Becker, M.; Berndt, R. Scattering and Lifetime Broadening of Quantum Well States in Pb Films on Ag(111). *Phys. Rev. B: Condens. Matter Mater. Phys.* **2010**, *81*, 205438.

(7) Park, J. S.; Quesada, A.; Meng, Y.; Li, J.; Jin, E.; Son, H.; Tan, A.; Wu, J.; Hwang, C.; Zhao, H. W.; et al. Determination of Spin-Polarized Quantum Well States and Spin-Split Energy Dispersions of Co Ultrathin Films Grown on Mo(110). *Phys. Rev. B: Condens. Matter Mater. Phys.* **2011**, *83*, 113405.

(8) Patthey, F.; Schneider, W.-D. Layer-by-Layer-Resolved Quantum-Well States in Ultrathin Silver Islands on Graphite: A Photoemission Study. *Phys. Rev. B: Condens. Matter Mater. Phys.* **1994**, *50*, 17560.

(9) Pacilé, D.; Leicht, P.; Papagno, M.; Sheverdyaeva, P. M.; Moras, P.; Carbone, C.; Krausert, K.; Zielke, L.; Fonin, M.; Dedkov, Y. S.; et al. J. Artificially Lattice-Mismatched Graphene/Metal Interface: Graphene/Ni/Ir(111). *Phys. Rev. B: Condens. Matter Mater. Phys.* **2013**, *87*, 035420.

(10) Nobis, D.; Potenz, M.; Niesner, D.; Fauster, T. Image-Potential States of Graphene on Noble-Metal Surfaces. *Phys. Rev. B: Condens. Matter Mater. Phys.* **2013**, *88*, 195435.

(11) Pacilé, D.; Lisi, S.; Di Bernardo, I.; Papagno, M.; Ferrari, L.; Pisarra, M.; Caputo, M.; Mahatha, S. K.; Sheverdyaeva, P. M.; Moras, P.; et al. Electronic Structure of Graphene/Co Interfaces. *Phys. Rev. B: Condens. Matter Mater. Phys.* **2014**, *90*, 195446.

(12) Jolie, W.; Craes, F.; Busse, C. Graphene on Weakly Interacting Metals: Dirac States versus Surface States. *Phys. Rev. B: Condens. Matter Mater. Phys.* **2015**, *91*, 115419.

(13) Leicht, P.; Zielke, L.; Bouvron, S.; Moroni, R.; Voloshina, E.; Hammerschmidt, L.; Dedkov, Y. S.; Fonin, M. In Situ Fabrication of Quasi-Free-Standing Epitaxial Graphene Nanoflakes on Gold. *ACS Nano* **2014**, *8*, 3735−3742.

(14) Tesch, J.; Leicht, P.; Blumenschein, F.; Gragnaniello, L.; Fonin, M.; Steinkasserer, L. E. M.; Paulus, B.; Voloshina, E.; Dedkov, Y. Structural and Electronic Properties of Graphene Nanoflakes on Au(111) and Ag(111). *Sci. Rep.* **2016**, *6*, 23439.

(15) Tesch, J.; Voloshina, E.; Jubitz, M.; Dedkov, Y.; Fonin, M. Local Electronic Properties of the Graphene-Protected Giant Rashba-Split $BiAg_2$ Surface. *Phys. Rev. B: Condens. Matter Mater. Phys.* **2017**, *95*, 155428.

(16) Alferov, Z. I. Nobel Lecture: The Double Heterostructure Concept and its Applications in Physics, Electronics, and Technology. *Rev. Mod. Phys.* **2001**, *73*, 767−782.

(17) https://www.elettra.trieste.it/it/lightsources/elettra/elettra-beamlines/vuv/vuvdescription.html.

(18) Klimovskikh, I.; Otrokov, M. M.; Voroshnin, V. Yu.; Sostina, D.; Petaccia, L.; Di Santo, G.; Thakur, S.; Chulkov, E. V.; Shikin, A. M. Spin-Orbit Coupling Induced Gap in Graphene on Pt(111) with Intercalated Pb Monolayer. *ACS Nano* **2017**, *11*, 368−374.

(19) Gao, M.; Pan, Y.; Huang, L.; Hu, H.; Zhang, L. Z.; Guo, H. M.; Du, S. X.; Gao, H.-J. Epitaxial Growth and Structural Property of Graphene on Pt(111). *Appl. Phys. Lett.* **2011**, *98*, 033101.

(20) Usachov, D.; Fedorov, A.; Otrokov, M. M.; Chikina, A.; Vilkov, O.; Petukhov, A.; Rybkin, A. G.; Koroteev, Y. M.; Chulkov, E. V.; Adamchuk, V. K.; et al. Observation of Single-Spin Dirac Fermions at the Graphene/Ferromagnet Interface. *Nano Lett.* **2015**, *15*, 2396−2401.

(21) Moras, P.; Wortmann, D.; Bihlmayer, G.; Ferrari, L.; Alejandro, G.; Zhou, P. H.; Topwal, D.; Sheverdyaeva, P. M.; Blügel, S.; Carbone, C. Probing the Electronic Transmission across a Buried Metal/Metal Interface. *Phys. Rev. B: Condens. Matter Mater. Phys.* **2010**, *82*, 155427.

(22) Shikin, A. M.; Vyalikh, D. V.; Dedkov, Yu. S.; Prudnikova, G. V.; Adamchuk, V. K.; Weschke, E.; Kaindl, G. Extended Energy Range of Ag Quantum-Well States in Ag(111)/Au(111)/W(110). *Phys. Rev. B: Condens. Matter Mater. Phys.* **2000**, *62*, R2303.

(23) Kralj, M. Hybridization Schemes for Ag Films on V(100). *Surf. Sci.* **2005**, *599*, 150−159.

(24) Varykhalov, A.; Shikin, A. M.; Gudat, W.; Moras, P.; Grazioli, C.; Carbone, C.; Rader, O. Probing the Ground State Electronic Structure of a Correlated Electron System by Quantum Well States: Ag/Ni(111). *Phys. Rev. Lett.* **2005**, *95*, 247601.

(25) Kliewer, J.; Berndt, R.; Chulkov, E. V.; Silkin, V. M.; Echenique, P. M.; Crampin, S. Dimensionality Effects in the Lifetime of Surface States. *Science* **2000**, *288*, 1399−1402.

(26) Paniago, R.; Matzdorf, R.; Meister, G.; Goldmann, A. Temperature Dependence of Shockley-type Surface Energy Bands on Cu(111), Ag(111) and Au(111). *Surf. Sci.* **1995**, *336*, 113−122.

(27) Varykhalov, A.; Marchenko, D.; Scholz, M. R.; Rienks, E. D. L.; Kim, T. K.; Bihlmayer, G.; Sánchez-Barriga, J.; Rader, O. Ir(111) Surface State with Giant Rashba Splitting Persists under Graphene in Air. *Phys. Rev. Lett.* **2012**, *108*, 066804.

(28) Neuhold, G.; Horn, K. Depopulation of the Ag(111) Surface State Assigned to Strain in Epitaxial Films. *Phys. Rev. Lett.* **1997**, *78*, 1327.

(29) Tomanic, T.; Sürgers, C.; Heid, R.; Alcántara Ortigoza, M.; Bohnen, K. ÐP.; Stöffler, D.; Löhneysen, H. v. Local-Strain Mapping on Ag(111) Islands on Nb(110). *Appl. Phys. Lett.* **2012**, *101*, 063111.

(30) Hövel, H.; Grimm, B.; Reihl, B. Modification of the Shockley-type Surface State on Ag(1 1 1) by an Adsorbed Xenon Layer. *Surf. Sci.* **2001**, *477*, 43−49.

DOI: 10.1021/acs.jpcc.8b09935
J. Phys. Chem. C 2019, 123, 9764−9769

(31) Papagno, M.; Moras, P.; Sheverdyaeva, P. M.; Doppler, J.; Garhofer, A.; Mittendorfer, F.; Redinger, J.; Carbone, C. Hybridization of Graphene and a Ag Monolayer Supported on Re(0001). *Phys. Rev. B: Condens. Matter Mater. Phys.* **2013**, *88*, 235430.
(32) Giovannetti, G.; Khomyakov, P. A.; Brocks, G.; Karpan, V. M.; van den Brink, J.; Kelly, P. J. Doping Graphene with Metal Contacts. *Phys. Rev. Lett.* **2008**, *101*, 026803.
(33) Khomyakov, P. A.; Giovannetti, G.; Rusu, P. C.; Brocks, G.; van den Brink, J.; Kelly, P. J. First-Principles Study of the Interaction and Charge Transfer Between Graphene and Metals. *Phys. Rev. B: Condens. Matter Mater. Phys.* **2009**, *79*, 195425.
(34) Vita, H.; Böttcher, S.; Horn, K.; Voloshina, E. N.; Ovcharenko, R. E.; Kampen, Th.; Thissen, A.; Dedkov, Yu. S. Understanding the Origin of Band Gap Formation in Graphene on Metals: Graphene on Cu/Ir(111). *Sci. Rep.* **2015**, *4*, 5704.
(35) Bostwick, A.; Ohta, T.; Seyller, T.; Horn, K.; Rotenberg, E. Quasiparticle Dynamics in Graphene. *Nat. Phys.* **2007**, *3*, 36−40.
(36) Zhou, S. Y.; Gweon, G. H.; Fedorov, A. V.; First, P. N.; de Heer, W. A.; Lee, D. H.; Guinea, F.; Castro Neto, A. H.; Lanzara, A. Substrate-Induced Bandgap Opening in Epitaxial Graphene. *Nat. Mater.* **2007**, *6*, 770−775.
(37) Rotenberg, E.; Bostwick, A.; Ohta, T.; McChesney, J. L.; Seyller, T.; Horn, K. Origin of the Energy Bandgap in Epitaxial Graphene. *Nat. Mater.* **2008**, *7*, 258−259.
(38) Zhou, S. Y.; Siegel, D. A.; Fedorov, A. V.; Gabaly, F. E.; Schmid, A. K.; Neto, A. H. C.; Lee, D.-H.; Lanzara, A. Origin of the Energy Bandgap in Epitaxial Graphene. *Nat. Mater.* **2008**, *7*, 259−260.
(39) Bostwick, A.; McChesney, J. L.; Emtsev, K. V.; Seyller, T.; Horn, K.; Kevan, S. D.; Rotenberg, E. Quasiparticle Transformation During a Metal Insulator Transition in Graphene. *Phys. Rev. Lett.* **2009**, *103*, 056404.
(40) Papagno, M.; Rusponi, S.; Sheverdyaeva, P. M.; Vlaic, S.; Etzkorn, M.; Pacilé, D.; Moras, P.; Carbone, C.; Brune, H. Large Band Gap Opening between Graphene Dirac Cones Induced by Na Adsorption onto an Ir Superlattice. *ACS Nano* **2012**, *6*, 199−204.
(41) Varykhalov, A.; Scholz, M. R.; Kim, T. K.; Rader, O. Effect of Noble-Metal Contacts on Doping and Band Gap of Graphene. *Phys. Rev. B: Condens. Matter Mater. Phys.* **2010**, *82*, No. 121101.
(42) Enderlein, C.; Kim, Y. S.; Bostwick, A.; Rotenberg, E.; Horn, K. The Formation of an Energy Gap in Graphene on Ruthenium by Controlling the Interface. *New J. Phys.* **2010**, *12*, 033014.
(43) Wallace, P. R. The Band Theory of Graphite. *Phys. Rev.* **1947**, *71*, 622.

DOI: 10.1021/acs.jpcc.8b09935
J. Phys. Chem. C 2019, 123, 9764−9769